International Journal of Mechanical, Industrial and Aerospace Sciences
ISSN: 2517-9950
Vol:8, No:10, 2014

3D Guidance of Unmanned Aerial Vehicles Using Sliding Mode Approach

M. Zamurad Shah, M. Kemal Özgören, Raza Samar

Abstract—This paper presents a 3D guidance scheme for Unmanned Aerial Vehicles (UAVs). The proposed guidance scheme is based on the sliding mode approach using nonlinear sliding manifolds. Generalized 3D kinematic equations are considered here during the design process to cater for the coupling between longitudinal and lateral motions. Sliding mode based guidance scheme is then derived for the multiple-input multiple-output (MIMO) system using the proposed nonlinear manifolds. Instead of traditional sliding surfaces, nonlinear sliding surfaces are proposed here for performance and stability in all flight conditions. In the reaching phase control inputs, the bang-bang terms with signum functions are accompanied with proportional terms in order to reduce the chattering amplitudes. The Proposed 3D guidance scheme is implemented on a 6-degrees-of-freedom (6-dof) simulation of a UAV and simulation results are presented here for different 3D trajectories with and without disturbances.

Keywords—Unmanned Aerial Vehicles, Sliding mode control, 3D Guidance, Path following, trajectory tracking, nonlinear sliding manifolds.

I. Introduction

THE reference trajectory is expressed in the form of lines and arcs in the 3D space in way-point guidance and the UAV has to follow it as closely as possible. Generally, longitudinal and lateral dynamics are decoupled during the guidance scheme design and two separate guidance schemes handle the deviations in longitudinal and lateral planes, respectively. For example, during the design of longitudinal guidance scheme, generally it is assumed that the vehicle bank/roll angle is zero. Similarly, it is assumed that the altitude and speed are held constant while designing the lateral guidance scheme. But generally it is not true and any guidance command in one plane have an effect on the other plane too. The main theme of this paper is derivation of a 3D guidance scheme that consider all these coupling effects and also the parametric/input disturbances.

The subject of fundamental guidance principles related to motion behaviour in a 2D plane and a 3D space is discussed in detail in [1]. Path generation and its tracking algorithm for UAVs in 3D space is discussed in [2]. The nonlinear path tracking algorithm resembles the line-of-sight guidance algorithm and lacks robustness in the presence of parametric uncertainties. In [3], authors address the problem of coordinated control of multiple UAVs in 3D space under tight spatial and temporal constraints. Similarly, the path-following problem of steering an autonomous vehicle along a desired path is discussed in [4], while tracking a predefined velocity profile. Both these algorithm rely on accurate measurement of velocity vector and any uncertainty in velocity is not taken care in the derivation. Backstepping based nonlinear guidance algorithm is proposed in [5] for UAVs 3D path tracking. The proposed guidance law assumes a very simple first order dynamics for heading and elevation angles, and the coupling between the two planes is ignored. For detailed discussion about 2D/3D guidance algorithms, interested readers are referred to [6].

Direct application of sliding mode control in the outer guidance loop is normally not feasible and discussed in detail in [7], [8]. In the authors' previous work [9], [10], [11], sliding mode based independent longitudinal and lateral guidance schemes of UAVs are discussed, and coupling between the two planes are ignored during the derivation of these guidance schemes. A novel nonlinear sliding surface for lateral guidance of UAVs is proposed in [9], and the proposed idea in detail along with experimental results is discussed in [10]. This work is the generalization of our previous work and a 3D guidance scheme for trajectory following of UAVs is proposed here. Generalized kinematic equations are considered here, and the problem becomes a guidance scheme for multiple-input multiple-out (MIMO) system due to coupling between the two planes. First, it is shown that traditional linear sliding manifolds are not a feasible solution for 3D trajectory following problem of UAVs, and nonlinear sliding manifolds are proposed here that give both performance and stability guarantee. Based on the proposed nonlinear sliding manifolds, a nonlinear guidance scheme is derived for the MIMO system. In order to reduce the chattering in control signal, bang-bang terms are accompanied with proportional terms in the reaching phase control design. The proposed guidance is implemented in 6-dof nonlinear simulation and different scenarios of flight are simulated. Simulation results in the absence and presence of disturbances are presented here to show the robustness of the proposed guidance scheme.

M. Zamurad Shah is researcher at the Department of Mechanical Engineering, Middle East Technical University, Ankara, Turkey. m.zamurad.2013@ieee.org

M. Kemal Özgören is with the Department of Mechanical Engineering, Middle East Technical University, Ankara, Turkey. ozgoren@metu.edu.tr

Raza Samar is with the Department of Electronic Engineering, Mohammad Ali Jinnah University, Islamabad, Pakistan. rsamar@jinnah.edu.pk

II. Problem Formulation

In literature, usually the 3D guidance problem is decoupled into two separate longitudinal and lateral guidance problems and coupling between longitudinal and lateral dynamics is ignored during the derivation of guidance logic. In this paper, we consider the generalized guidance problem of UAVs in three dimensional (3D) space. Kinematics and dynamics equations for aerospace vehicles are discussed in detail in many books and papers, e.g. [12], [13], [6]. Before the derivation of state equations for guidance logic design, first we introduce here the convention and notation of different variables.

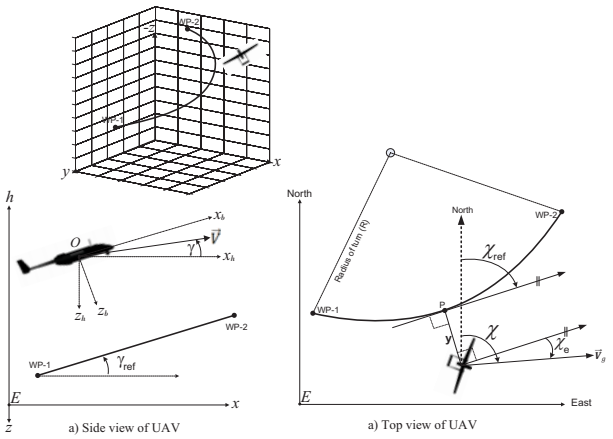

Fig. 1 Coordinate systems and their conventions

It is assumed that the earth is flat, non-rotating, and an approximate inertial reference frame. Standard convention of coordinate systems and their orientations ([13], [6]) is assumed here in this paper. The *body axes system* $Ox_by_bz_b$ is fixed to the UAV as shown in Fig. 1. The *ground axes system* $E_{xyz}(E_{NED})$ is fixed to the surface of the earth at mean sea level; where x, y and z are pointed towards *north*, *east* and *downward* directions, respectively. The *local horizontal system* $Ox_hy_hz_h$ moves with the airplane (O is the airplane center of gravity), but its axes remain parallel to the ground axes. In Fig. 1, all *axes systems* are shown from side and top views. Let $\overrightarrow{V}$ $(= \overrightarrow{V_g})$ and $\overrightarrow{V_a}$ denote the velocity vectors of the UAV relative to ground and relative to air respectively. Flight path angle γ denotes the orientation of ground velocity vector $(\overrightarrow{V})$ relative to the local horizon, and the course angle χ is orientation of ground velocity vector $(\overrightarrow{V})$ relative to the North. (x_N, x_E, h) is the position of UAV in 3D space.

The problem we address here in this paper is that of guiding a UAV from one waypoint to the next with minimum cross track and altitude deviations. Let $WP1(x_{N_1}, x_{E_1}, h_1)$ and $WP2(x_{N_2}, x_{E_2}, h_2)$ be two successive waypoints in 3D space as shown in Fig. 1. Looking from top view, let P be the nearest point to the vehicle on the arc and χ_{ref} be the angle of tangent line w.r.t. north at point P. Reference flight path angle γ_{ref} is the angle of desired path in the longitudinal plane. The cross track and altitude (normal) errors are denoted by y_e and h_e respectively. The main task of the guidance algorithm is to keep the errors (y_e and h_e) as small as possible.

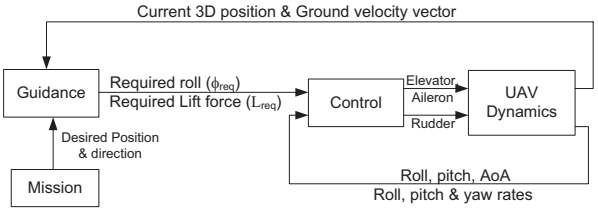

Fig. 2 Guidance and control structure

The approach used in this paper is based on separate design of the inner control loop and outer guidance loop. We will assume that the inner control loop is in place and we will focus on the guidance logic design. Fig. 2 shows the basic structure of guidance and control scheme. The outer guidance block gets current position and ground velocity vector $\overrightarrow{V}$ inputs from sensor and the reference path information from pre-planned mission plan (which can be modified during flight). On the basis of this information, the guidance block generates longitudinal and lateral acceleration commands for the inner control loop to follow. These longitudinal and lateral acceleration commands can also be represented by a reference angle of attack (α_{ref}) and a reference bank/roll angle (ϕ_{ref}) in case of bank-to-turn vehicles like UAVs. The inner control loop commands the control surfaces (elevators, aileron and vertical rudder) for following these reference commands. Here, we shall focus ourselves on the design of outer guidance logic that ensures tracking of the desired 3D path. This will be done using the sliding mode approach.

A. System Dynamics

Many flight mechanics books and papers [12], [13], [6] discuss the equations of motion for guidance and control of aerospace vehicles in detail. In this paper, we discuss it briefly and interested readers are referred to [6] for a detailed discussion. In 3D space, the forces acting on an aerospace vehicle during bank to turn and climb/decent maneuvers are summarized in Fig. 3. Summing up all the forces in the longitudinal and lateral planes, we have:

$$\begin{aligned} L\cos\phi &= mV\dot{\gamma} + mg\cos\gamma \\ L\sin\phi &= m(V\cos\gamma)\dot{\chi}, \end{aligned} \tag{1}$$

where L is the lift force, ϕ is the body roll angle, m is the mass, g is the gravitational acceleration and $V(= V_g)$ is the velocity of the vehicle relative to ground. Equation (1) can be written as:

$$\begin{aligned} \dot{\gamma} &= \frac{g}{V}\left(\frac{L\cos\phi}{mg} - \cos\gamma\right) \\ \dot{\chi} &= \frac{L\sin\phi}{mV\cos\gamma}, \end{aligned} \tag{2}$$

where γ and χ are the state variables. An important dimensionless term $\frac{L}{mg}$ in the above equation is known as the

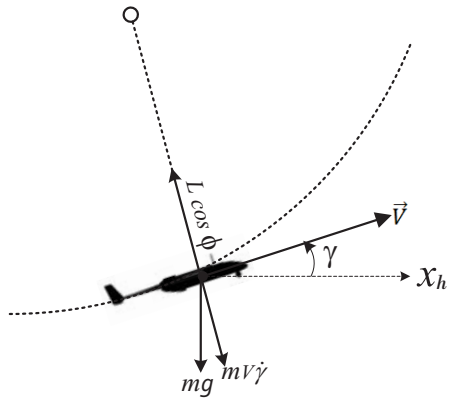

(a) side view during coordinated turn while climb/decent

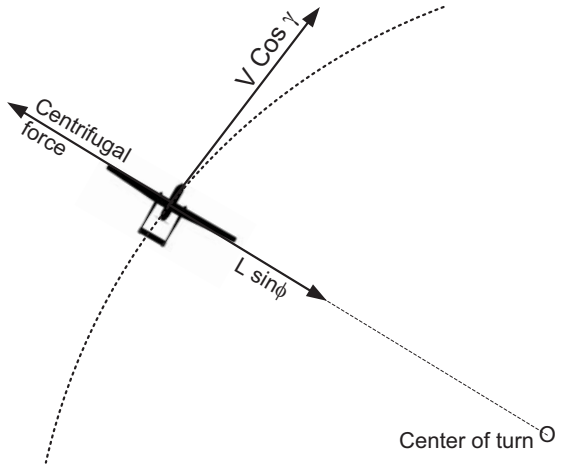

(b) Top view during coordinated turn while climb/decent

Fig. 3 Forces acting on a UAV during accelerating climb while coordinated turn

load factor, i.e. the number of normal $g's$ that an aerospace vehicle experiences during flight.

As the main theme of this paper is outer guidance loop design, so here we will make some assumptions related to the inner control loop. We assume here that: the inner control loop is already designed and it is fast enough (5-10 times faster than outer loop). Based on this assumption, we have $L_{req} \approx L$ and $\phi_{req} \approx \phi$, this implies that (2) can be approximated as:

$$\begin{aligned} \dot{\gamma} &= \frac{g}{V}\left(\frac{L_{req}\cos\phi_{req}}{mg} - \cos\gamma\right) \\ \dot{\chi} &= \frac{L_{req}\sin\phi_{req}}{mV\cos\gamma}. \end{aligned} \tag{3}$$

In these two equations, L_{req} (the required or reference Lift force) and ϕ_{req} (the required/reference roll angle) are the two control variables. These control variables are generated by outer guidance loop to follow the 3D path. Other state equations can be derived from the components of ground velocity (V). 3D position (x_N, x_E, h) of an aerospace vehicle in *ground axes system* E_{xyz} can be determined as:

$$\begin{aligned} \dot{x}_N &= (V\cos\gamma)\cos\chi, \quad \dot{x}_E = (V\cos\gamma)\sin\chi, \\ \dot{h} &= V\sin\gamma. \end{aligned} \tag{4}$$

These state equations can be written in error form. Let $WP1 - WP2$ be the desired path in 3D space as shown in Fig. 1, χ_{ref} and γ_{ref} are the desired course and flight path angles, respectively at any instance. Assuming $\chi_e = \chi - \chi_{ref}$ and $\gamma_e = \gamma - \gamma_{ref}$; we have the following state equations in error form:

$$\begin{aligned} \dot{h}_e &= V\sin\gamma_e \\ \dot{y}_e &= V\cos\gamma\sin\chi_e \\ \dot{\gamma}_e &= \frac{g}{V}\left(\frac{L_{req}\cos\phi_{req}}{mg} - \cos\gamma\right) - \dot{\gamma}_{ref} \\ \dot{\chi}_e &= \frac{L_{req}\sin\phi_{req}}{mV\cos\gamma} - \dot{\chi}_{ref}, \end{aligned} \tag{5}$$

where h_e (error in altitude perpendicular to the reference path), y_e (cross-track error), γ_e (error in flight path angle) and χ_e (error in course angle) are the four state variables. Control inputs are L_{req} (required Lift force) and ϕ_{req} (required roll angle), that the guidance loop has to generate for following the desired mission and bring back the vehicle back on the desired mission in case of any deviation.

III. Proposed Guidance Scheme

Sliding mode based control law design is a two step process in MIMO systems: the first step, stable sliding manifolds (number of sliding manifolds equal to the number of control inputs) are designed, and then a suitable control logic is designed to reach the sliding manifolds and maintain sliding motion for subsequent time despite the presence of model imprecision and disturbances [14], [15]. The idea is to force the trajectory of the system towards the sliding manifolds in the reaching phase, and once achieved, the system states must be constrained to remain on the sliding surfaces thereafter. Although sliding mode control has good robustness properties, one major difficulty is control chattering. Chattering is undesirable, since it involves extremely high frequency control activity, and furthermore may excite high-frequency neglected dynamics of the system. Saturation and sigmoid functions are commonly used as 'filters' to smoothen the discontinuous control signal so that it is realizable by mechanical hardware.

Linear sliding surfaces (i.e. linear combination of states) is commonly used as sliding manifolds but it is not feasible solution in every case. In the subsequent section, it is shown that a linear sliding surface is not a good choice for guidance law design of UAVs. Good performance for all scenarios as well as the stability of sliding surfaces are the main issues with linear sliding surfaces and hence non-linear sliding surfaces are proposed here for guidance logic design.

A. Proposed Sliding Manifolds

First, let us choose two linear sliding surface functions $s_1 = \gamma_e + \lambda_1 h_e$ and $s_2 = \chi_e + \lambda_2 y_e$ for some positive scalars λ_1 and λ_2 as shown in Fig. 4. In case of non-zero h_e, it is desired that $h_e \to 0$ as quickly as possible. Convergence of h_e to zero depends on the selection of λ_1, a bigger value of λ_1 gives fast convergence and is therefore desired for good performance. Similarly a larger value of λ_2 is also desirable for good performance in the lateral plane. On the other hand, sliding surfaces can become unstable for bigger values of λ_1 and λ_2. To see this it may be noted that motion on the sliding surface is described by $s_1 = 0$ and $s_2 = 0$ which yields $\gamma_e = -\lambda_1 h_e$ and $\chi_e = -\lambda_2 y_e$. After substitution in (5), we have:

$$\begin{aligned} \dot{h}_e &= -V \sin(\lambda_1 h_e), \\ \dot{y}_e &= -V \cos\gamma \sin(\lambda_2 y_e) \end{aligned} \tag{6}$$

For positive h_e, the term $\sin(\lambda_1 h_e)$ may be negative for large values of λ_1 and h_e. Hence $\dot{h}_e$ becomes positive for a positive h_e, implying instability. Similarly, $\dot{y}_e$ can be positive for a positive y_e and large λ_2, implying an unstable sliding surface. Both stability and performance is not possible with these linear sliding surfaces.

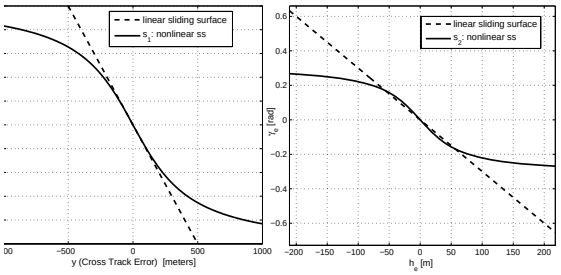

Fig. 4 Linear and proposed nonlinear sliding surfaces

In our previous work [10], [11], we proposed two independent nonlinear sliding surfaces for lateral and longitudinal guidance of UAVs. These sliding surfaces can be utilized here for 3D guidance of UAVs also. For good performance in all situations and stability of the sliding surfaces, we choose the following nonlinear sliding surfaces for 3D guidance of UAVs (see Fig. 4):

$$\begin{aligned} s_1 &= \chi_e + C_1 \arctan(C_2 y_e) = 0 \\ s_2 &= \gamma_e + C_3 \arctan(C_4 h_e) = 0 \end{aligned} \tag{7}$$

where the constants C_1, C_2, C_3 and C_4 are real positive numbers and $C_1, C_3 \leq 1$. Compared to the traditional linear sliding surfaces, here we have four parameters instead of two. For detailed discussion about these constants, interested readers are referred to the [10], [11].

Stability of the sliding manifolds:
Stability of the sliding surfaces proposed above can be proved using the equations of motion during sliding. Motion on the sliding surfaces is represented by $s_1 = 0$ and $s_2 = 0$, which implies $\chi_e = -C_1 \arctan(C_2 y_e)$ and $\gamma_e = -C_3 \arctan(C_4 h_e)$. Using (5), we have:

$$\begin{aligned} \dot{y}_e &= -V \sin\left[C_1 \arctan\left(C_2 y_e\right)\right] \cos\gamma, \\ \dot{h}_e &= -V \sin\left[C_3 \arctan\left(C_4 h_e\right)\right]. \end{aligned} \tag{8}$$

Here V and $\cos\gamma$ are positive variables. Since $C_1 \leq 1$, $\sin\left[C_1 \arctan\left(C_2 y_e\right)\right]$ is positive for any positive y_e, implying a negative $\dot{y}_e$, and vice-versa for negative y_e. Similarly, $\dot{h}_e$ is negative for positive h_e, and vice-versa. Once y_e and h_e will be zero, the other two state variable χ_e and γ_e will also be zero while sliding on the manifolds described in (7). Hence, we have two stable sliding surfaces and all state variables will converge to zero on the proposed nonlinear surfaces.

B. 3D Guidance Logic

After designing stable sliding manifolds, the next step is derivation of control law to reach the sliding manifolds and maintain motion on them subsequently. Generally, the control law is derived using the Lyapunov function $\mathbf{W} = \frac{1}{2}s^2$. A sliding phase control is derived from $\dot{s} = 0$ and then '$-k\,\mathrm{sgn}(s)$' is added to cater for uncertainties and un-modeled dynamics. To reduced chattering in the control signal, here we derive control law from $\dot{s} = -k_\triangle\,\mathrm{sgn}(s) - ks$. This yields:

$$\begin{aligned} \dot{\chi}_e + \frac{C_1 C_2}{1 + C_2^2 y_e^2}\dot{y} &= -k_{\triangle_1}\,\mathrm{sgn}(s_1) - k_1 s_1, \\ \dot{\gamma}_e + \frac{C_3 C_4}{1 + C_4^2 h_e^2}\dot{h}_e &= -k_{\triangle_2}\,\mathrm{sgn}(s_2) - k_2 s_2 \end{aligned} \tag{9}$$

or

$$\begin{aligned} \frac{L_{req}\sin\phi_{req}}{m\hat{V}\cos\gamma} - \dot{\chi}_{ref} + \frac{C_1 C_2}{1 + C_2^2 y_e^2}\hat{V}\cos\gamma\sin\chi_e \\ = -k_{\triangle_1}\,\mathrm{sgn}(s_1) - k_1 s_1, \\ \frac{L_{req}\cos\phi_{req}}{m\hat{V}} - \frac{g\cos\gamma}{\hat{V}} + \frac{C_3 C_4}{1 + C_4^2 h_e^2}\hat{V}\sin\gamma_e \\ -\dot{\gamma}_{ref} = -k_{\triangle_2}\,\mathrm{sgn}(s_2) - k_2 s_2, \end{aligned} \tag{10}$$

where $\hat{V}$ is the measured/estimated value of ground velocity V, and it is assumed here that all other parameters have negligible uncertainty (accurately measurable or known values). After rearranging the terms, we have the following expression for control variables $L_{req}\sin\phi_{req}$ and $L_{req}\cos\phi_{req}$:

$$\begin{aligned} L_{req}\sin\phi_{req} &= m\hat{V}\cos\gamma\Big(\frac{-C_1 C_2}{1 + C_2^2 y_e^2}\hat{V}\cos\gamma\sin\chi_e \\ &+ \dot{\chi}_{ref} - k_{\triangle_1}\,\mathrm{sgn}(s_1) - k_1 s_1\Big), \\ L_{req}\cos\phi_{req} &= m\hat{V}\Big(\frac{g\cos\gamma}{\hat{V}} - \frac{C_3 C_4}{1 + C_4^2 h_e^2}\hat{V}\sin\gamma_e \\ &+ \dot{\gamma}_{ref} - k_{\triangle_2}\,\mathrm{sgn}(s_2) - k_2 s_2\Big). \end{aligned} \tag{11}$$

These are the force components required in longitudinal and lateral inertial planes to keep the vehicle on track in 3D space.

These can easily be converted to L_{req} (required Lift force) and ϕ_{req} (required roll angle) to follow the desired mission. Also, L_{req} can be written in the form of α_{req} or θ_{req} as per the structure of the inner loop controller.

C. Reachability Condition

Using the global positive definite Lyapunov function $\mathbf{W} = \frac{1}{2}s^2$, condition on control variables $(k_{\triangle_1}, k_1, k_{\triangle_2}, k_2)$ can be derived to ensure reachability despite parametric uncertainties and disturbances. These feedback gains can be chosen so that $\dot{\mathbf{W}} = s\dot{s} < 0$ in the domain of attraction [14]. Here in the case of MIMO system:

$$s_1\dot{s_1} < 0 \quad \text{and} \quad s_2\dot{s_2} < 0. \tag{12}$$

These inequalities imply

$$s_1\left[\frac{L_{req}\sin\phi_{req}}{mV\cos\gamma} - \dot{\chi}_{ref} + \frac{C_1C_2}{1+C_2^2y_e^2}V\cos\gamma\sin\chi_e\right] < 0 \tag{13}$$
$$s_2\left[\frac{L_{req}\cos\phi_{req}}{mV} - \frac{g\cos\gamma}{V} + \frac{C_3C_4}{1+C_4^2h_e^2}V\sin\gamma_e - \dot{\gamma}_{ref}\right] < 0$$

Substituting values of control variables $L_{req}\sin\phi_{req}$ and $L_{req}\cos\phi_{req}$ from (11), we have:

$$\begin{aligned} s_1\Bigg[& \frac{\hat{V}}{V}\left(\frac{-C_1C_2}{1+C_2^2y_e^2}\hat{V}\cos\gamma\sin\chi_e + \dot{\chi}_{ref}\right) \\ & - \dot{\chi}_{ref} + \frac{C_1C_2}{1+C_2^2y_e^2}V\cos\gamma\sin\chi_e \\ & - \frac{\hat{V}}{V}k_{\triangle_1}\,\mathrm{sgn}(s_1) - \frac{\hat{V}}{V}k_1s_1\Bigg] < 0 \\ s_2\Bigg[& \frac{\hat{V}}{V}\left(\frac{-C_3C_4}{1+C_4^2h_e^2}\hat{V}\sin\gamma_e + \dot{\gamma}_{ref}\right) \\ & - \dot{\gamma}_{ref} + \frac{C_3C_4}{1+C_4^2h_e^2}V\sin\gamma_e \\ & - \frac{\hat{V}}{V}k_{\triangle_2}\,\mathrm{sgn}(s_2) - \frac{\hat{V}}{V}k_2s_2\Bigg] < 0 \end{aligned} \tag{14}$$

Assuming a maximum measurement uncertainty in $\hat{V}$ of $\tilde{V} = \hat{V} - V$, i.e. $\hat{V} = V + \tilde{V}$, (14) becomes:

$$\begin{aligned} s_1\Bigg[(2V+\tilde{V})\left(\frac{-C_1C_2}{1+C_2^2y_e^2}\tilde{V}\cos\gamma\sin\chi_e\right) + \tilde{V}\dot{\chi}_{ref} \\ -\hat{V}k_{\triangle_1}\,\mathrm{sgn}(s_1) - \hat{V}k_1s_1\Bigg] < 0 \\ s_2\Bigg[(2V+\tilde{V})\left(\frac{-C_3C_4}{1+C_4^2h_e^2}\tilde{V}\sin\gamma_e\right) + \tilde{V}\dot{\gamma}_{ref} \\ -\hat{V}k_{\triangle_2}\,\mathrm{sgn}(s_2) - \hat{V}k_2s_2\Bigg] < 0. \end{aligned} \tag{15}$$

The control variables $k_{\triangle_1}$ and $k_{\triangle_2}$ are designed to cater for parametric uncertainties; in other words, the left hand sides of (15) are negative definite, if

$$\begin{aligned} \hat{V}k_{\triangle_1} &> (2V+\tilde{V})\tfrac{C_1C_2}{1+C_2^2y_e^2}\tilde{V}\cos\gamma|\sin\chi_e| + \tilde{V}|\dot{\chi}_{ref}| \\ \hat{V}k_{\triangle_2} &> (2V+\tilde{V})\tfrac{C_3C_4}{1+C_4^2h_e^2}\tilde{V}|\sin\gamma_e| + \tilde{V}|\dot{\gamma}_{ref}| \end{aligned} \tag{16}$$

From implementation point of view, two options are possible: a simple option is to find the maximum value of these control gains for the extreme case and use these maximum control values in guidance logic, the other option is to keep the control gains adaptive and select their values depending on the state variable at every iteration. Here we have used the first strategy and in extreme case, we have:

$$\begin{aligned} k_{\triangle_1} &> \quad 0.707\tfrac{(2V_{max}+\tilde{V})\tilde{V}}{V_{min}}C_1C_2 + \tfrac{\tilde{V}}{V_{min}}|\dot{\chi}_{ref}| \\ k_{\triangle_2} &> \quad 0.707\tfrac{(2V_{max}+\tilde{V})\tilde{V}}{V_{min}}C_3C_4 + \tfrac{\tilde{V}}{V_{min}}|\dot{\gamma}_{ref}|. \end{aligned} \tag{17}$$

From above (17), it is clear that the control gains $k_{\triangle_1}$ and $k_{\triangle_2}$ are directly proportional to the uncertainty $\tilde{V}$ in velocity vector. The other control variables $k_1, k_2 > 0$ can be used for fast convergence towards sliding surface and a smooth control signal with less chattering.

IV. Simulation Results

Proposed 3D guidance scheme (11) is implemented in 6-dof nonlinear simulation of scaled YAK-54 UAV [9] and different scenarios are simulated. Nonlinear 6-dof simulation has complete nonlinear dynamics model of UAV [16] with option of different input disturbances like wind. Nonlinear dynamic model of the simulation is validated through flight experiments for different scenarios [10]. Sliding surface parameters C_1, C_2, C_3 and C_4 are chosen as 0.7, 0.007, 0.3 and 0.01, respectively. Control gains $k_{\triangle_1}$, $k_{\triangle_2}$, k_1 and k_2 are chosen as 50.0, 190.0, 120.0 and 100.0, respectively for implementation in simulation. Signum function ($\mathrm{sgn}(s)$) is approximated by $\frac{s}{|s|+\varepsilon}$ to avoid chattering in control signal. Proposed guidance law (11) generates required roll angle (ϕ_{req}) and required lift force (L_{req}). As per the structure of inner control loop, θ_r command is generated for the inner control loop using the relation $\theta = \alpha + \gamma$. Two cases are simulated and results are shown here:

A. Nominal case

Simulation results for a nominal pre-planned trajectory are shown in Fig. 5-7. In Fig. 5, reference and actual 3D trajectory of UAV are shown along with lateral and longitudinal errors. Maximum error in trajectory following is $\sim 2m$ in this case. Corresponding reference flight path and reference course angles are shown in Fig. 6 along with actual angles. Required pitch angle and required roll angle generated by the guidance loop are shown in Fig. 7 along with actual angles tracked by inner control loop.

B. With disturbances

The performance of the proposed guidance logic is evaluated in the presence of wind and GPS outage. An east wind of $4m/s$ is applied throughout in this case. Also, GPS

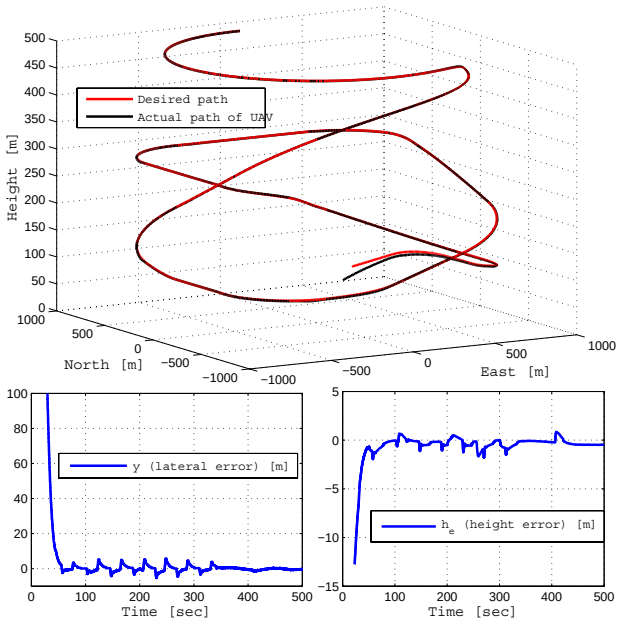

Fig. 5 Desired and achieved 3D trajectory of UAV

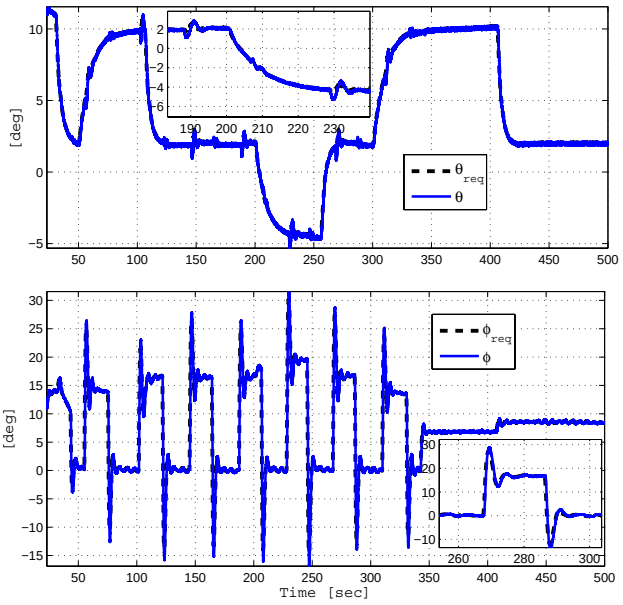

Fig. 7. Control inputs ϕ_{req} and θ_{req}, generated by proposed logic.

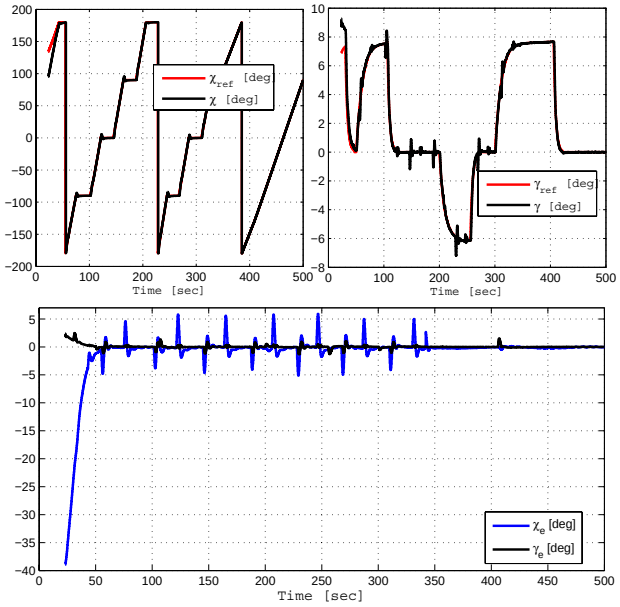

Fig. 6. Flight path and course angle of UAV.

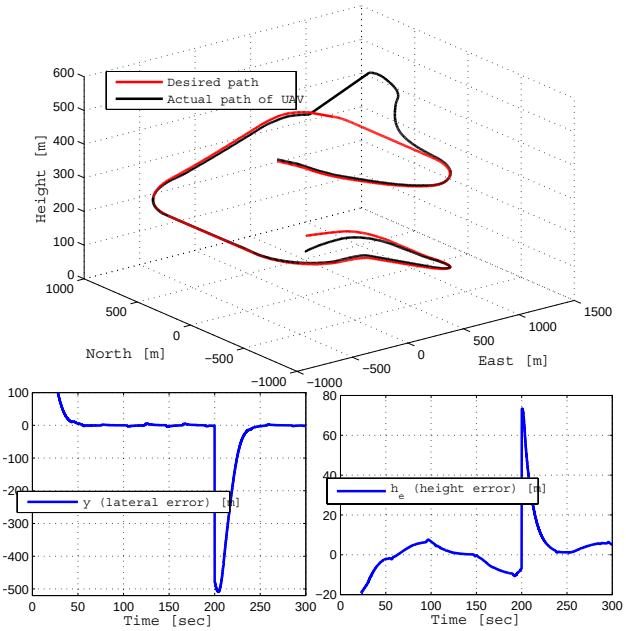

Fig. 8. Desired and achieved 3D trajectory of UAV.

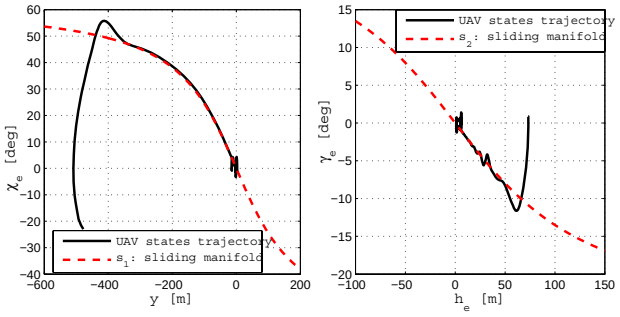

Fig. 9. Sliding motion on sliding manifolds.

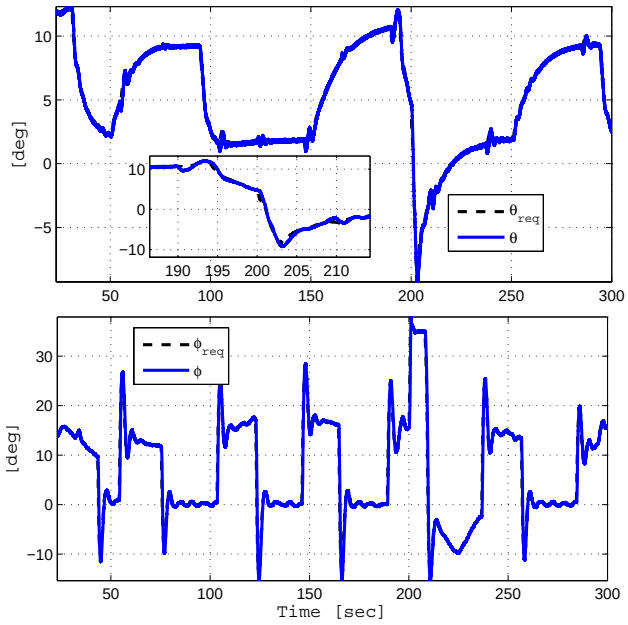

Fig. 10. Guidance scheme generated ϕ_{req} and θ_{req} for inner loop.

shows error in the position of UAV at $200s$ after few seconds outage. In Fig. 8, actual and desired trajectories are shown, the guidance logic bring back UAV on desired path successfully. In the presence of wind, the maximum steady state error in position is $\sim 10m$. In Fig. 9, motion of the states variable on the sliding surface is shown in the presence of wind. First, states trajectory is attracted towards the sliding surface and then maintained on it for subsequent time. Required pitch angle and required roll angle generated by the guidance loop are shown in Fig. 10.

V. Conclusions

In this paper, we generalized our previous 2D guidance scheme of UAVs for 3D space case. Instead of traditional decoupled longitudinal/lateral planes, here we used the generalized kinematics equations for guidance logic design. Based on these generalized equations, here we have a MIMO system that has two control variables. Based on two nonlinear sliding manifolds, a guidance scheme is proposed here for trajectory tracking of UAVs in 3D space. To reduce the chattering in control signal, a reaching control law that consists of bang-bang(signum function) and proportional terms is used here to reach and maintain the sliding motion. The Proposed 3D guidance scheme is implemented on a 6-degrees-of-freedom (6-dof) simulation of a UAV and simulation results are presented here for different 3D trajectories with/without disturbances. It is observed that the accuracy and smoothness requirements are fulfilled satisfactorily.

References

[1] M. Breivik, T. Fossen, Principles of guidance-based path following in 2d and 3d, in: Decision and Control, 2005 and 2005 European Control Conference. CDC-ECC '05. 44th IEEE Conference on, 2005, pp. 627–634. doi:10.1109/CDC.2005.1582226.

[2] G. Ambrosino, M. Ariola, U. Ciniglio, F. Corraro, E. De Lellis, A. Pironti, Path generation and tracking in 3-d for uavs, Control Systems Technology, IEEE Transactions on 17 (4) (2009) 980–988. doi:10.1109/TCST.2009.2014359.

[3] I. Kaminer, O. Yakimenko, A. Pascoal, R. Ghabcheloo, Path generation, path following and coordinated control for timecritical missions of multiple uavs, in: American Control Conference, 2006, 2006, pp. 4906–4913. doi:10.1109/ACC.2006.1657498.

[4] R. Cunha, C. Silvestre, A 3d path-following velocity-tracking controller for autonomous vehicles, in: Proceedings of the 16th IFAC World Congress, 2005, 2005. doi:10.3182/20050703-6-CZ-1902.02064.

[5] M. Ahmed, K. Subbarao, Nonlinear 3-d trajectory guidance for unmanned aerial vehicles, in: Control Automation Robotics Vision (ICARCV), 2010 11th International Conference on, 2010, pp. 1923–1927. doi:10.1109/ICARCV.2010.5707911.

[6] R. W. Beard, T. W. McLain, Small Unmanned Aircraft: Theory and Practice, Princeton University Press, 2012.

[7] Y. Shtessel, I. Shkolnikov, M. Brown, An asymptotic second-order smooth sliding mode control, Asian Journal of Control 4 (5) (2003) 959–967.

[8] Y. B. Shtessel, I. A. Shkolnikov, A. Levant, Smooth second-order sliding modes: Missile guidance application, Automatica 43 (8) (2007) 1470 – 1476. doi:10.1016/j.automatica.2007.01.008.

[9] M. Z. Shah, R. Samar, A. I. Bhatti, Lateral control for UAVs using sliding mode technique, in: 18^{th} IFAC World Congress, Milano, Italy, 2011.

[10] M. Z. Shah, R. Samar, A. Bhatti, Guidance of air vehicles: a sliding mode approach, Accepted for publication in IEEE Transactions on Control Systems Technology.

[11] M. Z. Shah, M. K. Özgören, R. Samar, Sliding mode based longitudinal guidance of UAVs, in: 2014 UKACC International Conference on Control (CONTROL), IEEE, 2014 (Accepted).

[12] A. Miele, Flight Mechanics: Theory of Flight Paths, no. 1. c. in Addison-Wesley Series in the engineering sciences, Elsevier Science & Technology, 1962.

[13] D. G. Hull, Fundamentals of Airplane Flight Mechanics, 1st Edition, Springer Publishing Company, Incorporated, 2007.

[14] C. Edwards, S. K. Spurgeon, Sliding Mode Control: Theory and Applications, Taylor and Francis, 1998.

[15] V. I. Utkin, Variable structure systems with sliding modes: a survey, IEEE Transactions on Automatic Control 22 (1977) 212–222.

[16] B. Stevens, F. Lewis, Aircraft Control & Simulation, 2nd Edition, Wiley and Sons, Hoboken, New Jersey, USA, 2003.